To Claude Bardos
from Sivaram

BOLTZMANN SCHEMES FOR CONTINUUM GAS DYNAMICS[1]

S.M.Deshpande

C.F.D.Laboratory, Department of Aerospace Engineering
Indian Institute of Science, Bangalore, India

1 Introduction

Many problems arising in the aircraft, launch vehicle and missile aerodynamics require the numerical solution of Euler Equations of Gas Dynamics and constructing numerical schemes for solving these equations has been one of the principal subjects of research among the CFD community for the last decade. The Euler Equations are nonlinear vector conservation equations and further are hyperbolic in nature. It has been found very essential from the point of view of accuracy and robustness to design numerical schemes which are conservative and upwind, that is, which respect hyperbolicity. Before the advent of the Boltzmann schemes upwinding has been enforced either via flux-vector splitting [1] or via flux difference splitting [2]. The third line of approach employed in constructing the upwind schemes is based on what the author [3] calls the *moment method strategy* which is based on the fact that the Euler Equations are suitable moments of the Boltzmann equation of Kinetic Theory of Gases. Several other workers have also exploited this connection between the Boltzmann equation and the Euler Equations for constructing the Boltzmann schemes [4,5,6,7,8]. The principal subject matter of the present paper is to survey several Boltzmann schemes developed by

[1]Keynote lecture delivered at the 5^{th} Asian Congress of Fluid Mechanics, 10-14 August, 1992, Taejon, Korea

the author and his coworkers and point out some promising future directions of research into the rapidly growing area of Boltzmann (or Kinetic) schemes.

2 Basic Theory of Boltzmann Schemes

Let us illustrate the basic idea with reference to 1-D unsteady Euler Equations

$$\frac{\partial U}{\partial t} + \frac{\partial G}{\partial x} = 0 \tag{1}$$

where U is the vector of conserved varibles, G is the flux-vector and are given by

$$U = \begin{bmatrix} \rho \\ \rho u \\ \rho e \end{bmatrix} \tag{2}$$

$$G = \begin{bmatrix} \rho u \\ p + \rho u^2 \\ (\rho e + p)\, u \end{bmatrix} \tag{3}$$

Here ρ = mass density, u = flud velocity, p = pressure, e = total energy per unit mass = $\frac{p}{\rho(\gamma-1)} + \frac{1}{2}u^2$. The equation (1) can be otained as Ψ-moment of the 1-D collisionless Boltzmann equation

$$\frac{\partial F}{\partial t} + v\frac{\partial F}{\partial x} = 0 \tag{4}$$

where F is the Maxwellian velocity distribution given by

$$F = \frac{\rho}{I_0}\sqrt{\frac{\beta}{\pi}} exp\left[-\beta\,(v-u)^2 - \frac{I}{I_0}\right] \tag{5}$$

$\beta = \frac{1}{2RT}$, R = Gas constant per unit mass, v = molecular velocity, I = internal energy variable corresponding to nontranslational degrees of freedom, and

$$I_0 = \frac{3-\gamma}{4\,(\gamma-1)\,\beta} \tag{6}$$

The moment function vector is defined by

$$\Psi = \left[1, v, I + \frac{v^2}{2}\right]^T \tag{7}$$

The Euler Equations (1) can then be cast in the compact form

$$\left(\Psi, \frac{\partial F}{\partial t} + v\frac{\partial F}{\partial x}\right) = 0 \tag{8}$$

where the (Ψ, f) is defined by

$$(\Psi, f) = \int_0^\infty dI \int_{-\infty}^\infty dv \Psi f(v) \tag{9}$$

2.1 KTFLIC Method

The equation (7) is the basis of many Kinetic schemes. One of the earliest schemes called Kinetic-Fluid-In-Cell (KTFLIC) method due to Deshpande and Raul [9] exploits the above connection the Euler Equations and the Boltzmann equation. To obtain the state update formulae for the KTFLIC let us consider 1-D interval $a \leq x \leq b$ which is assumed to be divided into cells. If a particle moves from $x \in C_i$ to $x' \in C_j$ during time interval Δt, then this particle will have molecular velocity $v = \frac{x'-x}{\Delta t}$. Hence the mass, momentum and energy transfer from cell C_i to C_j during Δt are given by

$$Ma(C_i \rightarrow C_j) = \int_{C_i} dx \int_{C_j} dx' \frac{F(x, x')}{\Delta t} \tag{10}$$

$$Mo(C_i \rightarrow C_j) = \int_{C_i} dx \int_{C_j} dx' \frac{(x' - x)}{\Delta t} \frac{F(x, x')}{\Delta t} \tag{11}$$

$$En(C_i \rightarrow C_j) = \int_{C_i} dx \int_{C_j} dx' \left[I_0 + \frac{(x' - x)^2}{2\Delta t^2}\right] \frac{F(x, x')}{\Delta t} \tag{12}$$

where

$$F(x, x') = \rho(x) \sqrt{\frac{\beta(x)}{\pi}} exp\left[-\beta(x)\left(\frac{x' - x}{\Delta t} - u(x)\right)^2\right] \tag{13}$$

At the end of the transport of mass, momentum and energy from all cells C_i to the cell C_j, we have

$$Ma(C_j) = \sum_{all\ i} Ma(C_i \rightarrow C_j)\,,\ Mo(C_j) = \sum_{all\ i} Mo(C_i \rightarrow C_j)\,,$$

$$En(C_j) = \sum_{all\ i} En(C_i \rightarrow C_j) \tag{14}$$

which are the state update formulae for the KTFLIC method. Deshpande and Raul [9] have used KTFLIC method for the 1-D shock propagation problem and the results are shown in Fig.1. A large number of mesh points (500) were required for crisp shock. The KTFLIC method is explicit, unconditionally stable, and first order accurate in space and time. It is a forerunner of Morton's Characteristic Galerkin Approach [10]. The method involves double integrals and these have to be computed numerically and hence the method is computationally very expensive. Also, extension to multidimensions involves some problems in dealing with boundary conditions and keeping track of several possibilities as a particle moves from any cell to any other cell.

2.2 Kinetic Numerical Method (KNM)

A faster version of KTFLIC is the Kinetic Numerical Method (KNM) which has the simple state update formulae

$$U_j^{n+1} = (\Psi, F^n(x_j - v\Delta t, v, I)) \tag{15}$$

where $F^n(x_j, v, I)$ is the local Maxwellian at the grid point x_j and time level n. Reitz [5] was the first one who developed this KNM and applied it to 1-D shock problem. Deshpande [11] has shown that the KNM satisfies the entropy condition, upwinding property and has TVD (Total Variation Diminishing) property. For the purpose of proving the satisfaction of the entropy condition, Deshpande [3] has used slightly modified H-function and flux-function H_v

$$H = \int\int \left(FlnF + \frac{5-3\gamma}{2(\gamma-1)} Fln\beta \right) dvdI$$

$$H_v = \int\int v \left(FlnF + \frac{5-3\gamma}{2(\gamma-1)} Fln\beta \right) dvdI \tag{16}$$

Developing higher order accurate versions of KNM is not a straightforward job. Difficulty arises due to the fact that the governing equations are (8) and not (4), hence it is not possible to construct higher order schemes for equation (8) by taking moments of higher order schemes of equation (4). We emphasize that $\frac{\partial F}{\partial t} + v\frac{\partial F}{\partial x} \neq 0$, in fact

$$\frac{\partial F}{\partial t}+v\frac{\partial F}{\partial x} = \left(\frac{\partial \rho}{\partial t} + v\frac{\partial \rho}{\partial x}\right)\frac{\partial F}{\partial \rho}+\left(\frac{\partial u}{\partial t} + v\frac{\partial u}{\partial x}\right)\frac{\partial F}{\partial u}+\left(\frac{\partial \beta}{\partial t} + v\frac{\partial \beta}{\partial x}\right)\frac{\partial F}{\partial \beta} \quad (17)$$

The right hand side of equation (16) is very characteristic of the Chapman-Enskog theory. Replacing the time derivatives of ρ, u, β in terms of space derivatives using the Euler Equations we get

$$\frac{\partial F}{\partial t} + v\frac{\partial F}{\partial x} = P_{CE}F \quad (18)$$

where P_{CE} is the Chapman-Enskog polynomial and is given by

$$P_{CE} = \frac{\partial u}{\partial x}P_\tau + \frac{\partial \beta}{\partial x}P_q \quad (19)$$

$$P_\tau = \frac{3\gamma - 5}{2} + (3-\gamma)\frac{(v-u)^2}{2RT} - \frac{4(\gamma-1)^2}{3-\gamma}\frac{I}{2RT} \quad (20)$$

$$P_q = 5RT(v-u) - \frac{4(\gamma-1)}{3-\gamma}I(v-u) - (v-u)^3 \quad (21)$$

The Chapman-Enskog polynomial has the interesting property

$$(\Psi,\ P_{CE}F) = 0 \quad (22)$$

We are now ready to construct the second order accurate KNM of Deshpande [11,12]. Start with

$$U^{n+1} = \left(\Psi, F^{n+1}\right) = (\Psi, F^n) + \Delta t\left(\Psi, \frac{\partial F^n}{\partial t}\right) + \frac{\Delta t^2}{2}\left(\Psi, \frac{\partial^2 F^n}{\partial t^2}\right) + \ldots$$

Using the equation (17) we obtain

$$U^{n+1} = (\Psi, F^n) - \Delta t\left(\Psi, v\frac{\partial F^n}{\partial x}\right) + \Delta t^2\left(\Psi, \frac{\partial^2 F^n}{\partial t^2}\right) + \ldots \quad (23)$$

where we have used equations (18) and (22). For the second derivative $\frac{\partial^2 F}{\partial t^2}$ we have

$$\frac{\partial^2 F}{\partial t^2} = -v\frac{\partial}{\partial x}\left(\frac{\partial F}{\partial t}\right) + \frac{\partial}{\partial t}\left(P_{CE}F\right)$$

$$= +v^2\frac{\partial^2 F}{\partial x^2} - v\frac{\partial}{\partial x}\left(P_{CE}F\right) + \frac{\partial}{\partial t}\left(P_{CE}F\right)$$

Substituting in (23) and after some rearrangement we get

$$U^{n+1} = \left(\Psi, F^n\left(x - v\Delta t\right)\right) - \frac{\Delta t^2}{2}\left(\Psi, v\frac{\partial}{\partial x}P_{CE}F\right) + O\left(\Delta t^3\right) \qquad (24)$$

which shows that in addition to $F^n\left(x - v\Delta t\right)$ term we have one more term containing the Chapman-Enskog polynomial. Hence the Maxwellian distribution alone will not yield a second order accurate KNM. Defining

$$f_{CE} = F\left(1 + \frac{\Delta t}{2}P_{CE}\right) \qquad (25)$$

the equation (24) can also be recast as

$$U^{n+1} = \left(\Psi, f^n_{CE}\left(x - v\Delta t\right)\right) + O\left(\Delta t^3\right) \qquad (26)$$

When equation (25) is compared with the usual Chapman-Enskog distribution

$$f_{CE} = F\left(1 - \frac{\tau}{p}P_\tau - \frac{q\sqrt{3}}{p}P_q\right)$$

we observe that the distribution (25) is antidiffusive showing that such antidiffusive terms are necessary to achieve second order accuracy. Fig.2 shows the density and velocity plots for 1-D shock propagation problem solved by using the state update formula (26). Slope limiters [3] have been used to suppress wiggles. It is observed that the KNM yields accurate results with high resolution.

3 The Kinetic Flux Vector Splitting (KFVS) Scheme

The KNM involves only one numerical integration with respect to space variable and is therefore faster than KTFLIC method. It is tempting to enhance the speed further by modifying KNM, and this can be accomplished

by reducing its support. This brings us to the Kinetic Flux Vector Splitting (KFVS) scheme of Deshpande [11] and Mandal and Deshpande [12]. The KFVS method is obtained by splitting the Maxwellian into two parts corresponding to $v > 0$ and $v < 0$. The flux-vector G therefore splits as

$$G^+ = \left(\Psi, \frac{v + |v|}{2} F\right) \quad and \; G^- = \left(\Psi, \frac{v - |v|}{2} F\right) \tag{27}$$

The split flux-vectors G^+ and G^- are integrals of $vF\Psi$ over positive and negative half spaces in velocity v. They can be evaluated in closed form in terms of error functions as

$$G^{\pm} = \begin{bmatrix} \rho u A^{\pm} \pm \rho B \\ (p + \rho u^2) A^{\pm} \pm \rho u B \\ (pu + \rho u e) A^{\pm} \pm \left(\frac{p}{2} + \rho \mathbf{e}\right) B \end{bmatrix} \tag{28}$$

where

$$A^{\pm} = \frac{1 \pm erfs}{2} \;, \; B = \frac{e^{-s^2}}{2\sqrt{\pi\beta}} \; and \; s = speed \; ratio = u\sqrt{\beta}$$

In terms of the split fluxes the Euler Equations become

$$\frac{\partial U}{\partial t} + \frac{\partial G^+}{\partial x} + \frac{\partial G^-}{\partial x} = 0 \tag{29}$$

Upwind differencing the split-flux terms in equation (29) we obtain the first order KFVS scheme

$$\left(\frac{\partial U}{\partial t}\right)_j^n + \frac{G_j^{+n} - G_{j-1}^{+n}}{\Delta x} + \frac{G_{j+1}^{-n} - G_j^{-n}}{\Delta x} = 0 \tag{30}$$

Substituting for U, G^+ and G^- in terms of F we get

$$\frac{\partial}{\partial t}\left(\Psi, F_j^n\right)$$

$$+ \frac{1}{\Delta x}\left(\Psi, \frac{v + |v|}{2}\left(F_j^n - F_{j-1}^n\right)\right) + \frac{1}{\Delta x}\left(\Psi, \frac{v - |v|}{2}\left(F_{j+1}^n - F_j^n\right)\right) = 0$$

which is obviously the Ψ-moment of the CIR differenced Boltzmann equation

$$\left(\frac{\partial F}{\partial t}\right)_j^n + \frac{v+|v|}{2}\frac{F_j^n - F_{j-1}^n}{\Delta x} + \frac{v-|v|}{2}\frac{F_{j+1}^n - F_j^n}{\Delta x} = 0 \qquad (31)$$

Now an interesting question arises whether the KFVS scheme (30) which is obtained from (31) remains an upwind scheme after moments are taken. In order to demonstrate that the scheme (30) obtained by differencing (29) is an upwind scheme it is necessary to transform equation (29) to a symmetric hyperbolic form. Deshpande [13] has shown that equation (29) can be transformed to

$$P\frac{\partial q}{\partial t} + B^+\frac{\partial q}{\partial x} + B^-\frac{\partial q}{\partial x} = 0 \qquad (32)$$

where q is the transformed vector given by

$$q = \left[ln\rho + \frac{ln\beta}{\gamma - 1} - \beta u^2, 2\beta u, -2\beta\right]^T$$

P=positive symmetric matrix, and B^+, B^- are positive and negative symmetric matrices respectively. It then follows that $P^{-1}B^+$ and $P^{-1}B^-$ have real positive and real negative eigenvalues respectively, thus justifying the backward differencing of $B^+\frac{\partial q}{\partial x}$ and forward differencing of $B^+\frac{\partial q}{\partial x}$. It has been found that the eigenvalues of $P^{-1}B^+$ and $P^{-1}B^-$ are smooth functions of the Mach number [12].

Mandal and Deshpande [12] have shown that the above KFVS scheme can be made higher order accurate by following the analysis of Chakravarthy and Osher [14]. For this purpose we write the KFVS in the form

$$\left(\frac{\partial U}{\partial t}\right)_j^n + \frac{G_{j+\frac{1}{2}}^n - G_{j-\frac{1}{2}}^n}{\Delta x} = 0 \qquad (33)$$

The first order KFVS given by (30) is obtained by choosing

$$G_{j+\frac{1}{2}} = \frac{G_j + G_{j+1}}{2} + \frac{DG^-_{j+\frac{1}{2}} - DG^-_{j-\frac{1}{2}}}{2} \qquad (34)$$

where the flux differences $DG^{\pm}_{j+\frac{1}{2}}$ are defined by

$$DG^{\pm}_{j+\frac{1}{2}} = \left(\Psi, \frac{v \pm |v|}{2}(F_{j+1} - F_j)\right) = \frac{\left(G^{\pm}_{j+1} - G^{\pm}_j\right)}{2} \qquad (35)$$

The equations (33) and (34) express the KFVS scheme in a flux-difference splitting format implying that the KFVS scheme can also be looked upon as a flux-difference splitting scheme. Higher order schemes can now be obtained by modifying the formulae for $G_{j+\frac{1}{2}}$ as

$$G_{j+\frac{1}{2}} = EFS$$

$$+ \frac{1}{4}\left[(1+\phi)\left(DG^{+}_{j+\frac{1}{2}} - DG^{-}_{j+\frac{1}{2}}\right) + (1-\phi)\left(DG^{+}_{j-\frac{1}{2}} - DG^{-}_{j+\frac{3}{2}}\right)\right] \qquad (36)$$

where EFS is the right hand side of the equation (34) representing the expressions for the first order scheme. The parameter ϕ takes on respectively the values -1 and $\frac{1}{3}$ for the second and third order upwind schemes. In order to suppress the spurious wiggles in the solution it is necessary to introduce the modified differences

$$\tilde{DG}^{\pm}_{j+\frac{1}{2}} = minmod\left[DG^{\pm}_{j+\frac{1}{2}}, \tilde{R} \times DG^{\pm}_{j-\frac{1}{2}}\right]. \qquad (37)$$

$$\tilde{\tilde{DG}}^{\pm}_{j+\frac{1}{2}} = minmod\left[DG^{\pm}_{j+\frac{1}{2}}, \tilde{R} \times DG^{\pm}_{j+\frac{3}{2}}\right] \qquad (38)$$

where $\tilde{R}$ is a limiter with $0 \leq \tilde{R} \leq \frac{3-\phi}{1-\phi}$ and

$$minmod\,[a,b] = \frac{sgn\,(a) + sgn\,(b)}{2} min\,[|a|,|b|] \qquad (39)$$

$$sgn\,(a) = +1\ if\ a > 0,\ -1\ if\ a < 0,\ 0.0\ if\ a = 0.0 \qquad (40)$$

With this modified differences the formula (36) becomes

$$G_{j+\frac{1}{2}} = EFS$$

$$+ \frac{1}{4}\left[(1+\phi)\left(\tilde{DG}^{+}_{j+\frac{1}{2}} - \tilde{\tilde{DG}}^{-}_{j+\frac{1}{2}}\right) + (1-\phi)\left(\tilde{\tilde{DG}}^{+}_{j-\frac{1}{2}} - \tilde{\tilde{DG}}^{-}_{j+\frac{3}{2}}\right)\right] \qquad (41)$$

Fig.3 shows the computed density and fluid velocity profiles using the first order, second order and third order KFVS schemes for which $G_{j+\frac{1}{2}}$ given by equations (34) and (41) are used. The accuracy of the results and the crispness of the shock are evident.

4 KFVS Applied to Multidimensional Flows

After having proven the capability of the KFVS method for a 1-D test case it is necessary to find out how it performs on 2-D and 3-D flows for low subsonic to hypersonic Mach numbers. Mandal [15] has applied the high resolution finite volume KFVS method to the standard test cases of shock reflection and bump in a channel problems. Figures 4 to 9 show the pressure contours and residue history for these problems. Mathur *et al.* [16] have applied the first order as well as high resolution KFVS schemes to a variety of 2-D problems with structured and unstructured meshes. They have used cell centered finite volume KFVS method. In order to use the high resolution KFVS method (which is a must in transonic regime) on a triangular mesh it is necessary to obtain the fluxes on the edges of a cell using extrapolation. Consider for example, a cell centre P of a triangular cell whose edges are shown hatched in the sketch below :

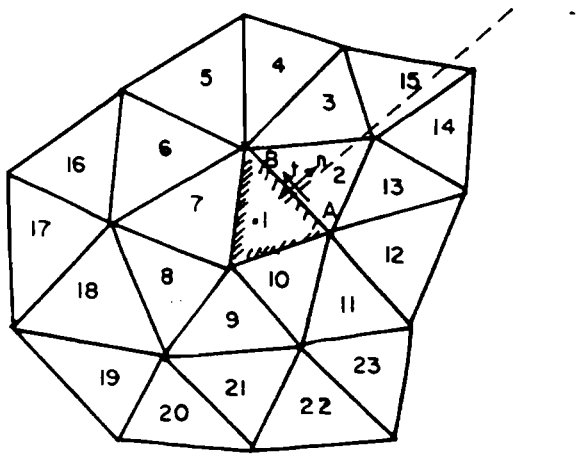

The problem is to find out the flux on the edge AB in conformity with the upwinding principle. Let n be the outward normal to AB and t tangent to the edge. Then applying the usual upwinding criterion we get

$$G_{AB} = G^{+}\left(u_{n1}, u_{t1}\right) + G^{-}\left(u_{n2}, u_{t2}\right) \tag{42}$$

Here we have suppressed the dependence of G^{+} and G^{-} on density and temperature. In obtaining G_{AB} as above we have used only the data at cell centres 1 and 2. In order to obtain high resolution KFVS it is necessary to

use the data at other neighbouring cell centres. Mathur *et al.* [16] consider the cell centres 13,14,15 and 3 and select that cell centre of this set which is closest to the straight line joining the centres 1 and 2. Assuming that this centre is 15, the flux G^-_{AB} is then obtained by extrapolation based on G^-_2 and G^-_{15}. By using the same criterion G^+_{AB} can also be obtained. Obviously to suppress the wiggles minmod operators as explained before need to be used. Figures 10 and 11 show typical results obtained by Mathur *et al.* for the flow past an airfoil and flow through a ramp in a channel. They have made extensive comparisons between the results obtained by KFVS and Jameson's methods and concluded that KFVS method performs as well as Jameson's method and some times better.

Recently Deshpande *et al.* [17] have developed a 3-D time marching Euler code (calledd BHEEMA) using the KFVS method for computing high speed flows around hypersonic reentry configuration consisting of cone-cylinder-flares and control surfaces. This code uses finite volume method and operates on a hexahedral mesh generated by using the stacked grids. Figures 12 and 13 show the pressure contours for axisymmetric configuration at M = 4 and $\alpha = 2°$, and plot of pressure coefficient for the reentry configuration with wings at $M = 1°$ and $\alpha = 0°$. Based on an elaborate comparison of the aerodynamic coefficients (C_A, C_N, C_M etc.) obtained from BHEEMA with the wind tunnel results they conclude that the time marching 3-D Euler code BHEEMA is a reliable design tool for predicting aerodynamic coefficients within 15%. Recently Dass and Deshpande [18] have successfully used the convergence acceleration device GMRES in combination with KFVS for obtaining faster convergence.

As a last example of the application of KFVS mention may be made of the work of Teerthamalai and Deshpande [19] who computed hypersonic reacting flow over a hemisphere using KFVS method and equilibrium chemistry model. For this purpose they considered 5 species (O, N, NO, O_2, N_2) and 3 reactions model

$$R_1 : O_2 + M \rightleftharpoons 2O + M,$$

$$R_2 : N_2 + M \rightleftharpoons 2N + M,$$

$$R_3 : N_2 + O_2 \rightleftharpoons 2NO.$$

For a specified γ the Euler Equations were solved by BHEEMA for computing density, fluid velocity and temperature everywhere in the flow field. Then

the chemistry module was used compute mass fractions, temperature and γ everywhere in the flow field. The results of the computations reveal that the drag coefficient for Mach 10,15,20 was within 2% of that obtained by using the nonreacting perfect gas model. However, the temperature differs substantially. Figures 14 and 15 show the temperature and pressure contours for $M_\infty = 10,20$.

It is therefore reasonable to conclude that the KFVS method has travelled a long way since its modest beginning in 1982 and is now a fully tested and validated Kinetic upwind method capable of computing inviscid compressible flows past any configuration.

5 Promising Future Directions

Search is continuously on for the elusive best method for obtaining numerical solution of the Euler Equations. The two guiding principles for developing new methods demand that the method be less dissipative compared to the existing ones and further that it should mimic the physics of the flow as much as possible. The development of upwind schemes is a consequence of following the second principle. We discuss briefly here four new ideas for developing upwind schemes exploiting the connection between the Boltzmann equation and the Euler Equations.

5.1 Use of Exponential Switch

Considering 1-D problem again for the sake of demonstrating the idea we observe that KFVS is equivalent to assuming that the flux at the boundary B of a cell (see the sketch below) is given by

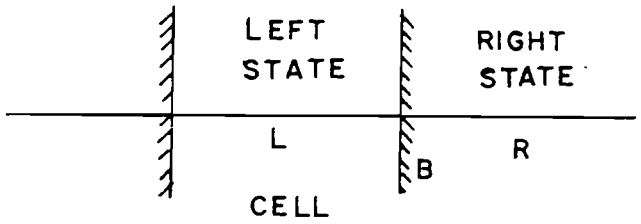

$$f_B = \frac{F_R + F_L}{2} - \frac{F_R - F_L}{2} sgn(v) \tag{43}$$

Here F_R and F_L are the Maxwellians corresponding to the right and left states respectively and sgn(v) is the usual sign function. We now replace the sign function by the exponential function giving

$$f_B = \frac{F_R + F_L}{2} - \frac{F_R - F_L}{2} exp\left(-\frac{\alpha|v|\Delta t}{\Delta x}\right) \quad for\ v \geq 0$$

$$f_B = \frac{F_R + F_L}{2} + \frac{F_R - F_L}{2} exp\left(-\frac{\alpha|v|\Delta t}{\Delta x}\right) \quad for\ v \leq 0 \tag{44}$$

where α is a nonnegative real number. When the controlling parameter α is zero we get the standard KFVS scheme and when α is infinity we obtain the central difference scheme which has zero diffusion. Thus by continuously varying α we can control the numerical diffusion in the scheme. Raghurama Rao and Deshpande [20] have applied the above scheme to 1-D shock tube problem. The results are shown in Fig.16 from which it is obvious that the above modification does reduce the diffusion in the scheme. Further investigation is essential to develop the idea even more.

5.2 Kinetic Splitting Based on Thermal Velocity

One of the criticisms that may be raised against the KFVS is that the method assumes the existence of the rest frame as the splitting of the flux requires the division of velocity space into two halves $v \geq 0$ and $v \leq 0$. As the rest frame is physically meaningless it may be a good idea to do the splitting without assuming the existence of a rest frame. One possibility is to do the splitting based on the thermal (or what is also called as peculiar) velocity. The thermal velocity $\vec{c}$ appears in the formulae for pressure, temperature and stress tensor of the Kinetic Theory of Gases, and is thus physically more meaningful than the variable $\vec{v}$. The motion of a molecule can be thought of as consisting of a random movement with velocity c superimposed on an orderly motion with velocity u. The random variable c is a Gaussianly distributed variable if we are dealing with inviscid gas dynamics. It may therefore be rewarding if a numerical scheme is constructed exploiting the

above ideas. For the present we do splitting based on c. Towards this end we write the collisionless Boltzmann equation in the form

$$\frac{\partial F}{\partial t} + u\frac{\partial F}{\partial x} + c\frac{\partial F}{\partial x} = 0 \tag{45}$$

Taking the moments we obtain

$$\frac{\partial U}{\partial t} + \frac{\partial G^t}{\partial x} + \frac{\partial G^a}{\partial x} = 0 \tag{46}$$

where

$$G^t = (u\Psi, F) = \begin{bmatrix} \rho u \\ \rho u^2 \\ eu \end{bmatrix} \text{ and } G^a = (c\Psi, F) = \begin{bmatrix} 0 \\ p \\ pu \end{bmatrix} \tag{47}$$

The eigenvalues of the flux Jacobian $\frac{\partial G^t}{\partial U}$ are all u,u,u showing that $\frac{\partial G^t}{\partial x}$ corresponds to the transport of fluid with velocity u. The eigenvalues of $\frac{\partial G^a}{\partial U}$ on the other hand are 0, $\pm a\sqrt{(\gamma-1)/\gamma}$ where a is the local sonic velocity. The dynamics of the fluid can therefore be considered as being influenced partly by the particle motion (movement with velocity u) and partly by the wave motion (random movement or movement of waves with velocity 0, $\pm a\sqrt{(\gamma-1)/\gamma}$. Balakrishnan and Deshpande [21] were the first ones who experimented with numerical schemes exploiting the wave-particle behaviour of fluid motion. Here we are attacking the problem from a different angle, namely, the construction of the Boltzmann scheme by treating the u and c terms differently. Following Raghurama Rao and Deshpande [20] we split G^a into G^{a+} and G^{a-} defined by

$$G^{a+} = \left(\Psi, \frac{c+|c|}{2}F\right) \text{ and } G^{a-} = \left(\Psi, \frac{c-|c|}{2}F\right) \tag{48}$$

which can be simplified as

$$G^{a\pm} = \begin{bmatrix} \pm\frac{\rho}{2\sqrt{\pi\beta}} \\ \frac{p}{2} \pm \frac{\rho u}{2\sqrt{\pi\beta}} \\ \frac{pu}{2} \pm \frac{1}{2\sqrt{\pi\beta}}\left(\frac{p}{2} + \rho\epsilon\right) \end{bmatrix} \tag{49}$$

Raghurama Rao and Deshpande [20] have solved the 1-D shock tube problem and 2-D shock reflection problem using the above upwind method (which they term as Kinetic Acoustic Flux Vector Splitting - KAFVS scheme). Figures 17 and 18 show the results obtained. Even though the 1-D results do not show significant reduction in the dissipation, the 2-D computations using KAFVS show much less smearing of the shock than the KFVS method. Further, KAFVS is found to be much less expensive compared to the KFVS method. The basic idea of treating uf_x and cf_x terms in a different fashion seems quite sound and definitely needs much more study and testing on a variety of multidimensional problems.

5.3 Multidirectional Boltzmann Schemes

Many multidimensional upwind schemes advance the solution through a sequence of one-dimensional operators. The underlying physical model therefore involves wave propagation only along coordinate directions while the physical situation is that the waves propagate along all possible directions. Powell and Van Leer [22] have observed that the inability to take the physics properly into account leads to the numerical schemes mentioned above to be strongly coupled to the grid on which they operate. Thus there is a need to design grid independent numerical schemes. Raghurama Rao and Deshpande [23] have developed a genuinely multidimensional upwind Boltzmann scheme. Following the recent terminology this method can also be called as Multidirectional Upwind Boltzmann Scheme.

Consider the collisionless Boltzmann equation

$$\frac{\partial f}{\partial t} + \vec{v} \cdot \frac{\partial f}{\partial \vec{x}} = 0 \tag{50}$$

Considering a 2-D flow, the central problem in developing a multidirectional upwind scheme for the Euler Equations (via the moment method strategy) is to develop a suitable discrete approximation to $v_1 \frac{\partial f}{\partial x} + v_2 \frac{\partial f}{\partial x}$ on the quadrilateral mesh, a portion of which is shown in the sketch that follows.

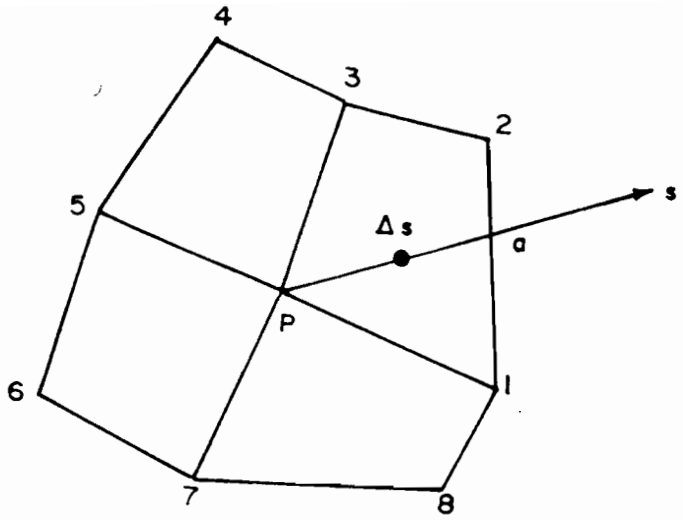

The mesh point P is surrounded by eight mesh points. Particles arrive at P from all directions and not just along coordinate directions x and y since the molecular velocities v_1, v_2 vary from $-\infty$ to $+\infty$. The problem then boils down to obtain a finite difference approximation to $\vec{v} \cdot grad\ f$ for each $\vec{v}$. Keeping in mind that $\vec{v} \cdot grad\ f = v\frac{\partial f}{\partial s}$, where s = coordinate along $\vec{v}$, we can obtain the first order finite difference approximation as

$$v\frac{\partial f}{\partial s} = v\frac{f_P - f_Q}{\Delta s} \tag{51}$$

where Δs = Distance between the points P and Q. We notice that on the right hand side of equation (51) the difference $f_P - f_Q$ appears instead of $f_Q - f_P$ because particles having velocity antiparallel to direction s send information to P. A slight rearrangement of equation (51) yields

$$v\frac{\partial f}{\partial s} = \left(v\frac{\Delta n}{\Delta s}\right)\frac{f_P - f_Q}{\Delta n} = v_n\frac{f_P - f_Q}{\Delta n} \tag{52}$$

The next problem is to calculate f_Q from the data at the nodes 1,2,...,8. The position of the donor point Q depends on the velocities (v_1, v_2) and could be anywhere on any of the eight segments 12,23,...,81. Consider the segment 12. Assuming linear variation between the nodes 1 and 2 the distribution function f_Q could be computed easily. Raghurama Rao and Dehspande [23] have given all the details involved in interpolation, obtaining appropriate limits of integration with respect to v_1, v_2. Of the two integrations they have been able to perform one, while the other one has to be performed numerically. Integrations with respect to velocities v_1, v_2 appear in the formulation when we pass from equation (51) to the Euler Equations via the moment method

strategy. As the resultant scheme takes into account all possible directions it is aptly called as multidirectional upwind Boltzmann scheme. They have applied this scheme to the standard shock reflection problem and the results are shown in Fig.19 where the pressure contours from this scheme are compared with those from the usual KFVS scheme. It is obvious that the multidirectional scheme has much less smearing. Unfortunately, this multidirectional scheme is very expensive and further research is necessary to improve it. Constructing a new multidirectional scheme using the thermal velocity is an attractive idea.

5.4 Least Squares Weak Upwind Scheme

Presently development of Euler Solvers on unstructured meshes is mostly limited to finite element and finite volume based methods. The use of unstructured grid with finite difference formulation is still a challenging task. Recently Deshpande, Mandal and Ghosh [24,25] have tackled this problem from a completely different point of view. At the heart of this formulation is the least squares discrete approximation to the derivatives f_x and f_y of any function f which in the present case is the Maxwellian velocity distribution

$$f = F = \frac{\rho}{2\pi RT} exp\left[-\frac{(v_1 - u_1)^2}{2RT} - \frac{(v_1 - u_1)^2}{2RT} - \frac{I}{I_0}\right] \tag{53}$$

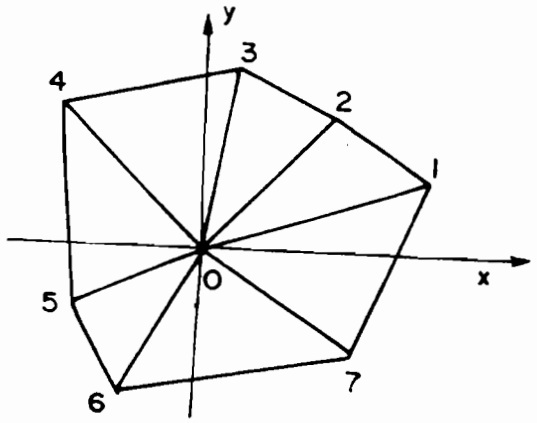

Let us consider a part of the triangular mesh shown in the above figure where the node 0 is surrounded by nodes 1,2,3,... and let x_i, y_i be the coordinates of the node i. Introduce the notation

$$\Delta f_i = f_i - f_o,\ \Delta x_i = x_i - x_o,\ \Delta y_i = y_i - y_o$$

The Taylor expansion gives

$$\Delta f_i = f_{xo}\Delta x_i + f_{yo}\Delta y_i,\ i = 1, 2, \ldots, n \tag{54}$$

Thus we have two unknowns f_{xo} and f_{yo} and n linear equations. By minimizing the square of the error

$$e = \sum_{i=1}^{n} (\Delta f_i - f_{xo}\Delta x_i - f_{yo}\Delta y_i)^2 \tag{55}$$

we get the least squares approximation

$$f_{xo} = \frac{\| \Delta y \|^2 (\Delta x, \Delta f) - (\Delta x, \Delta y)(\Delta y, \Delta f)}{\| \Delta x \|^2 \| \Delta y \|^2 - (\Delta x, \Delta y)^2} \tag{56}$$

$$f_{yo} = \frac{\| \Delta y \|^2 (\Delta y, \Delta f) - (\Delta x, \Delta y)(\Delta x, \Delta f)}{\| \Delta x \|^2 \| \Delta y \|^2 - (\Delta x, \Delta y)^2} \tag{57}$$

where

$$\| \Delta x \|^2 = \sum_{i=1}^{n} \Delta x_i^2,\ \| \Delta y \|^2 = \sum_{i=1}^{n} \Delta y_i^2,$$

$$(\Delta x, \Delta f) = \sum_{i=1}^{n} \Delta x_i \Delta f_i,\ (\Delta y, \Delta f) = \sum_{i=1}^{n} \Delta y_i \Delta f_i \tag{58}$$

The formulae (56) and (57) are only first order accurate and the second order accurate least squares approximations are obtained by replacing Δf_i in (56) and (57) by $\Delta \tilde{f}_i$ defined by

$$\Delta \tilde{f}_i = \Delta f_i - \frac{1}{2}\Delta x_i \Delta f_{xi} - \frac{1}{2}\Delta y_i \Delta f_{yi},\ \Delta f_{xi} = f_{xo} - f_{xi},\ \Delta f_{yi} = f_{yo} - f_{yi} \tag{59}$$

An upwind scheme for the solution of the 2-D Boltzmann equation

$$\frac{\partial f}{\partial t} + v_1 \frac{\partial f}{\partial x} + v_2 \frac{\partial f}{\partial y} = 0 \tag{60}$$

Acknowledgements

The work presented in this paper is based on the research work done by several graduate students at the CFD Laboratory of the Department of Aerospace Engineering, Indian Institute of Science, Bangalore, India and collobborators from Research and Development organisations within the country. The author is specially thankful to Mandal, J.C., Raghurama Rao, S.V., Ghosh, A.K., Nagarathinam, M., Sekar, S.,Krishnamurthy, R., Sinha, P.K. and Kulkarni, P.S.. The financial support obtained from Indo-Soviet Integrated Long Term Programme of Coordination in Science and Technology and Indo-French Centre for the Promotion of Advanced Research (IFCPAR)/Centre FRanco-Indien pour la Promotion de la Recherche ADvancé (CFIPRA) are gratefully acknowledged.

References

1 Van Leer, B., 'Flux Vector Splitting for the Euler Equations', Lecture Notes in Physics, 1982, vol.170, pp 507-512, Springer verlag.

2 Roe, P.L., 'Approximate Riemann Solvers, Parameter Vectors and Difference Schemes', Journal of Comp. Phys., 1981, vol.43, No.2, pp 357-372.

3 Deshpande, S.M., 'A Second Order Accurate Kinetic Theory Based Method for Inviscid Compressible Flows', NASA Technical Paper 2613, 1986.

4 Pullin, D.L., 'Direct Simulation Methods for Compressible Inviscid Ideal Gas Flows', Journal of Comp. Phy., 1980, vol.34, no.2, pp 231-244.

5 Rietz,R.D., 'One-Dimensional Compressible Gas Dynamics Calculations using the Boltzmann Equation', Journal of Comp. Phys., 1981, vol.42, no.1, pp 108-123.

6 Perthame, B. 'Boltzmann Type Schemes for Gas Dynamics and the Entropy Property', SIAM Journal of Numerical Analysis, 1990, vol.27, No.6, pp 1405-1421.

7 Elizarova, T.G. and Chetverrushkin, B.N., 'Kinetic Algorithms for Calculating Gas Dynamic Flows', Journal of Comput. Math. and Math. Phys., 1985, vol.25, no.10, pp 1526-1533.

8 Kaniel, S., 'A Kinetic Model for the Compressible Flow Equations', Indiana Univ. Mathematics J., 1988, 37, pp 537-563.

9 Deshpande, S.M. and Raul, R., 'Kinetic Theory Based Fluid-in-Cell Method for Eulerian Fluid Dynamics', 82 FM 14, Fluid Mechanics report, Department of Aerospace Engineering, Indian Institute of Science, Bangalore, India, 1982.

10 Morton, K.W., 'Generalized Galerkin Methods for Nonlinear Hyperbolic Problems', Computer methods in App. Mech. and Engg., 1985, 52, pp 835-859.

11 Deshpande, S.M., 'Kinetic Theory based New Upwind Methods for Inviscid Compressible Flows', AIAA Paper 86-0275, 1986.

12 Mandal, J.C. and Deshpande, S.M., 'Higher Order Accurate Kinitic Flux Vector Splitting Method for Euler Equations', Proceedings of the Second International Conference on Nonlinear Hyperbolic Problems', Aachen, FRG, March 14-18, 1988. Also in Notes on Numerical Fluid Mechanics, vol.24, vieweg, Bramschweig, 1989.

13 Deshpande, S.M., 'On the Maxwellian Distribution, Symmetric Form, and Energy Conservation for the Euler Equations', NASA Technical Paper 2583, 1986.

14 Chakravarthy, S.R. and Osher, S., 'High Resolution Applications of the Osher Upwind Scheme for the Euler Equations', AIAA paper no. 83-1913, 1983.

15 Mandal,J.C., 'Kinetic Upwind Method for Inviscid Compressible Flows', Ph.D. thesis, Department of Aerospace Engineering, Indian Institute of Science, Bangalore, India, 1989.

16 Mathur, J.S., Natakasumah, D.K., Marchant, M.J. and Weatherill, N.P., 'An Upwind Kinetic Flux Vector Splitting Method for the Euler Equations on Different Grid Types', C'C.A.E. 1004, January, 1992.

Institute for Numerical Methods in Engineering, University College of Swansea, UK.

17 Deshpande, S.M., Sekar, S., Nagarathinam, M., Krishnamurthy, R., Sinha, P.K. and Kulkarni, P.S., 'A 3-Dimensional Upwind Euler Solver Using Kinetic Flux Vector Splitting Method', presented at 13^{th} International Conference on Numerical Methods in Fluid Dynamics, Rome, 6-10 July, 1992.

18 Deshpande, S.M. and Dass, A.K., 'GMRES Acceleration of Kinetic Flux Vector Split Euler Code', accepted for presentation in the First European Conference on Computational Fluid Dynamics to be held in Brussels, 7-11 September, 1992.

19 Theerthamalai, P. and Deshpande, S.M., 'Computation of Hypersonic Flows Over a Spherer Using Kinetic Flux Vector Splitting Scheme', submitted to 6^{th} National Conference on Aerodynamics to be held in Aeronautical Development Establishment, Bangalore, during 23-25 September, 1992.

20 Raghurama Rao, S.V. and Deshpande, S.M., 'A Class of Low Dissipation Kinetic Upwind Schemes for Inviscid Compressible Flows', 91 FM 11, Fluid Mechanics reports, Department of Aerospace Engineering, Indian Institute of Science, Bangalore, India, 1991.

21 Balakrishnan, N. and Deshpande, S.M., 'New Upwind Schemes with Wave-Particle Splitting for Inviscid Compressible Flows', 91 FM 12, Fluid Mechanics reports, Department of Aerospace Engineering, Indian Institute of Science, Bangalore, India, 1991.

22 Powell, K.G. and Van Leer, B., 'A Genuinely Multidimensional Upwind Cell-Vertex Scheme for the Euler Equations', AIAA Paper 89-0095, 1989.

23 Raghurama Rao, S.V. and Deshpande, S.M., 'A Genuinely Multi dimensional Upwind Boltzmann Scheme for Euler Equations', 91 FM 6, Fluid Mechanics Reports, Department of Aerospace Engineerng, Indian Institute of Science, Bangalore, India, 1991.

21 Deshpande, S.M., Mandal, J.C. and Ghosh, A.K., 'Kinetic Upwind Method for Inviscid Gas Dynamics', presented at Common Wealth Advisory Aeronautical Research Council (CAARC) Specialists Meeting on CFD during 5-10 December, 1988, National Aeronautical Laboratory, Bangalore, India.

25 Deshpande, S.M., Ghosh, A.K. and Mandal, J.C., 'Least Squares Weak Upwind Method for Euler Equations', 89 FM 4, Fluid Mechanics report, Department of Aerospace Engineering, Indian Institute of Science, Bangalore, India, 1989.

N = 300 ARTVISE=0.00000 NCELL = 500 DELTA = $1X10^{-6}$ CHART = 500

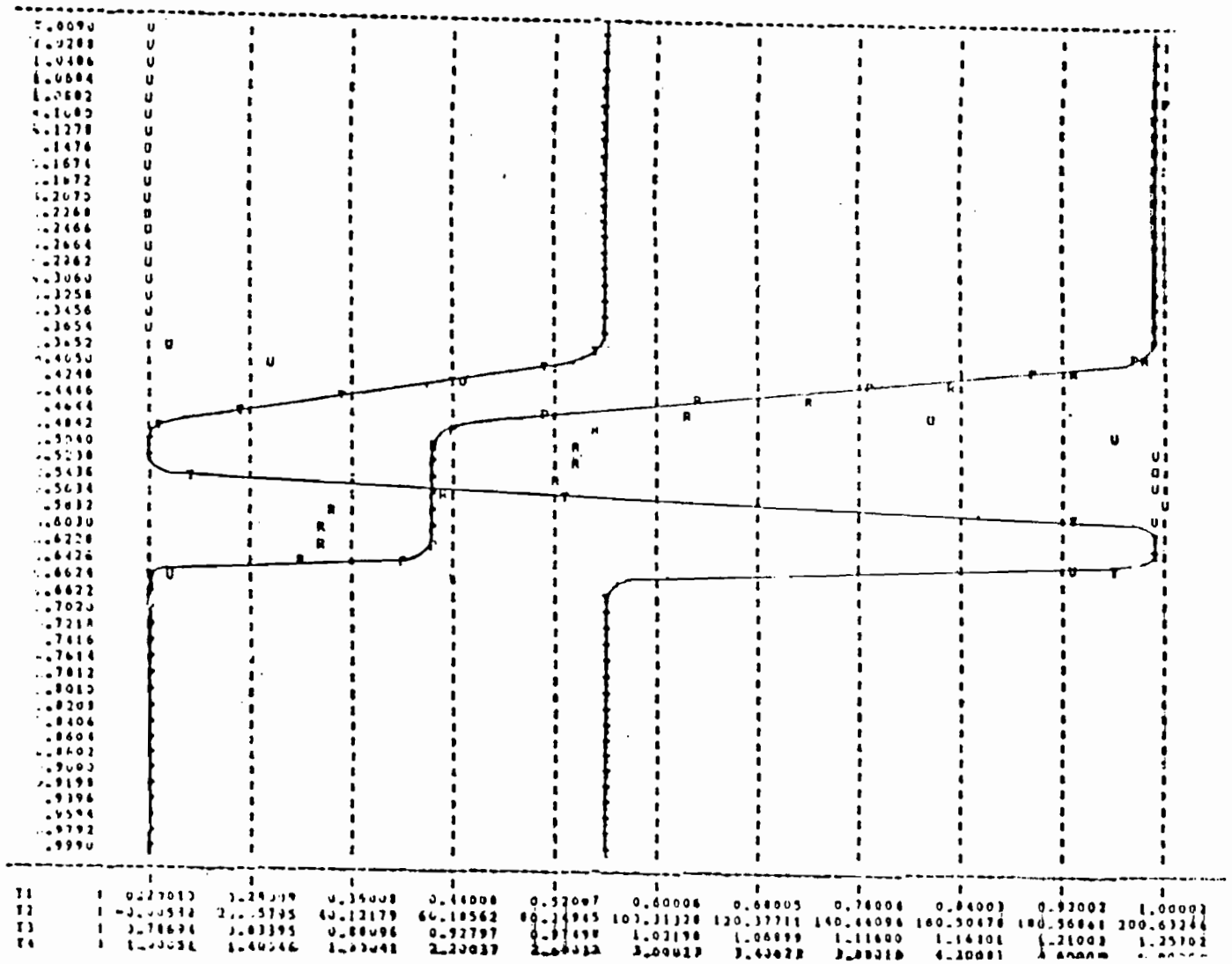

Fig.1 Application of KFLIC to 1-D Shock Propagation Problem

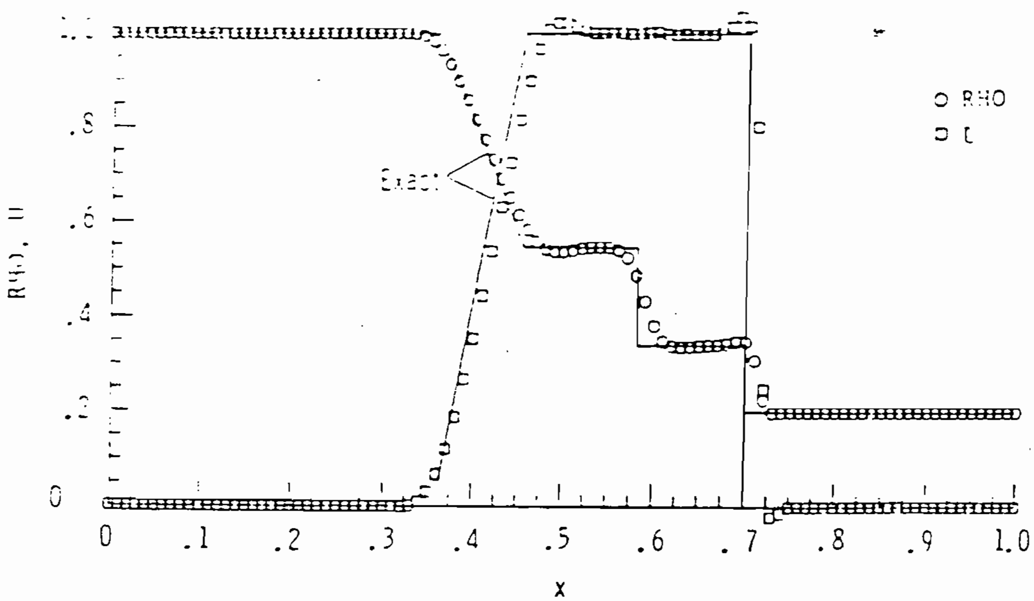

Fig.2 Computed and exact RHO and U profiles for shock tube problem with chapman-Enskog ansatz with T.V.D modification $J = 101$; $t_A = 0.00041$ Sec.

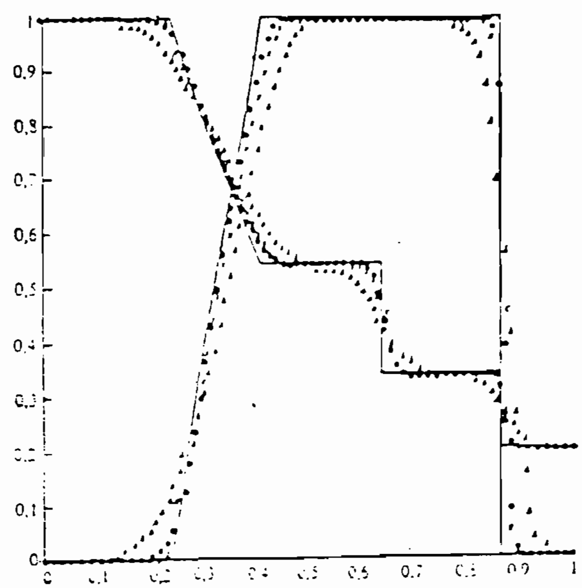

Fig.3 Computed RHO, U and exact(–) profiles for shock tube [illegible] UVFS. First order (△), second [illegible] order [illegible]

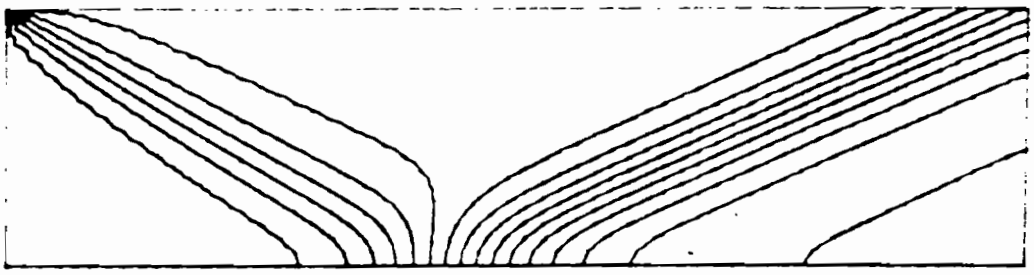

Contours from [illegible] with an interval 0.2

Fig. 4 Pressure contours for shock reflection problem at supersonic Mach number (M_∞ =2.9, oblique shock angle=29°) obtained using first order time marching finite difference KFVS scheme

a

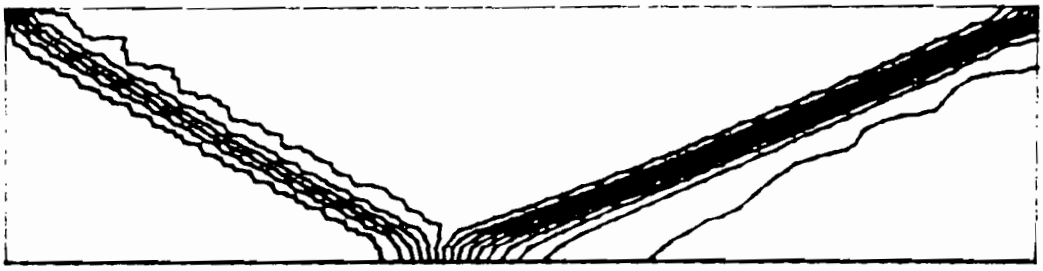

b

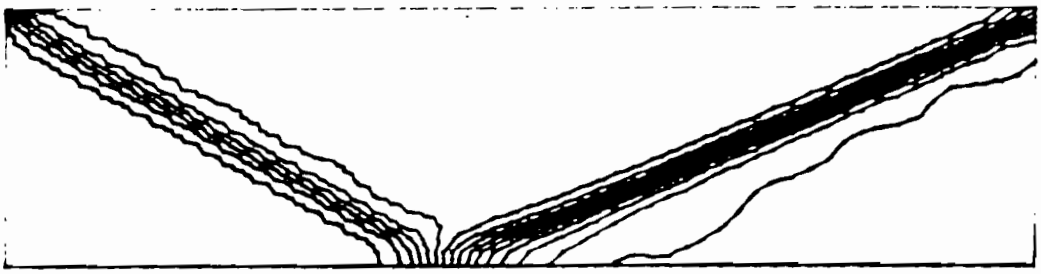

Contours from 0.9 to 4.1 with an interval 0.2

Fig. 5 Pressure contours for shock reflection problem at supersonic Mach number (M_∞=2.9,oblique shock angle=29°) obtained using (b) second order and (c) third order time marching finite difference KFVS scheme

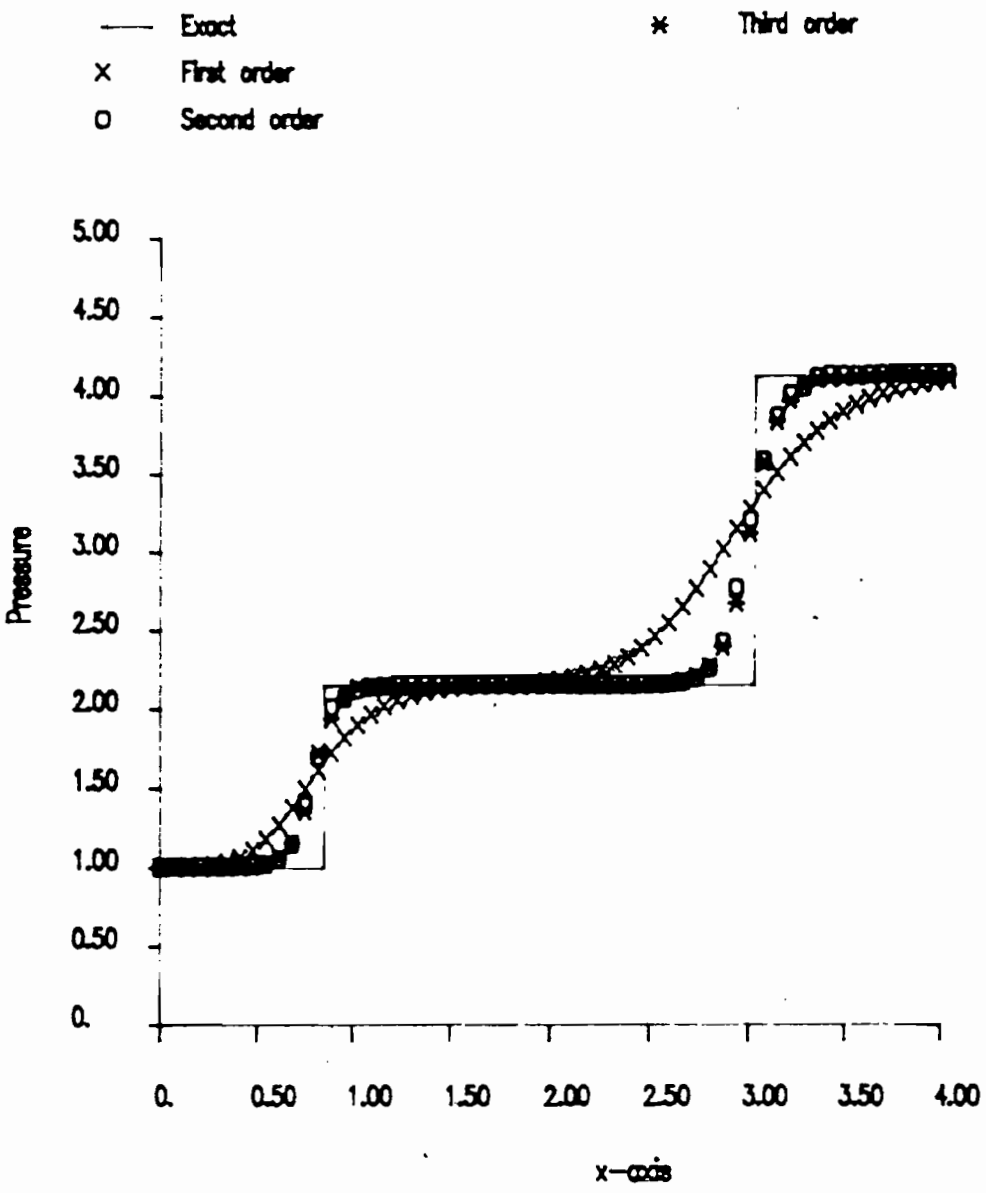

Fig. 6 Pressure distribution at y=0.5 computed using first, second and third order time marching finite difference KFVS schemes

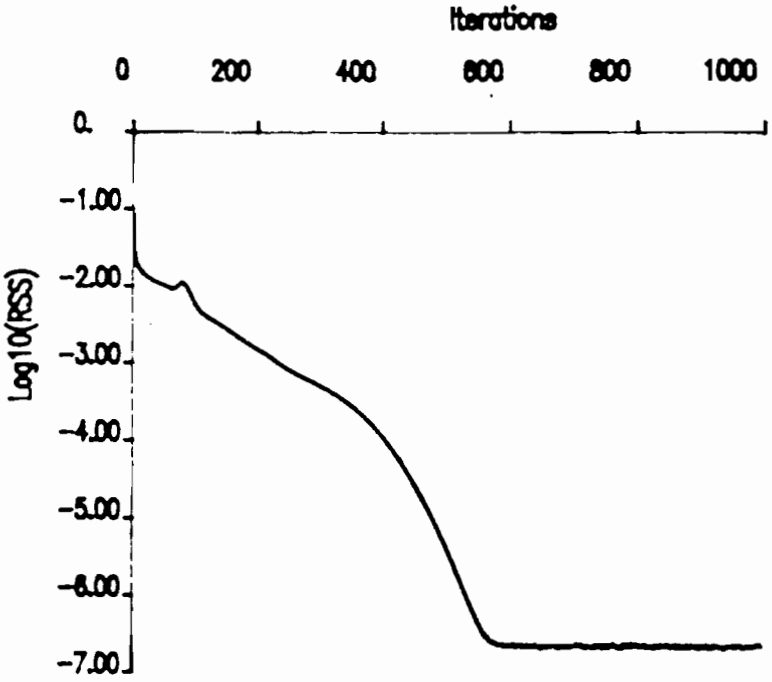

Fig. 7 Convergence history for the shock reflection problem at supersonic Mach number using first order time marching finite difference KFVS scheme.

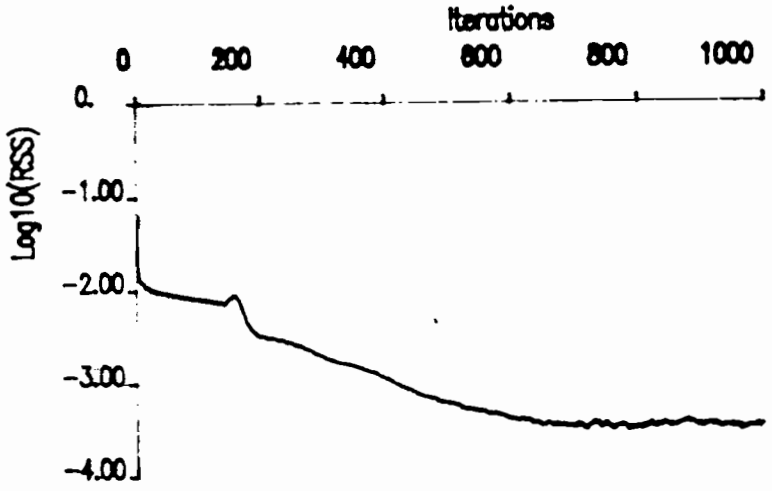

Fig. 8 Convergence history for the shock reflection problem at supersonic Mach number using second order time marching finite difference scheme.

(a)

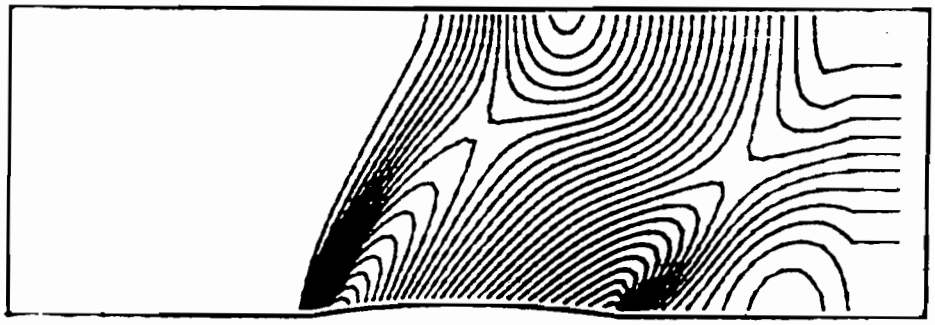

(b)

Contours from 0.65 to 1.45 with an interval 0.025.

Fig. 9 Pressure contours for supersonic flow (M_∞ = 1.4) over a 4% thick circular arc bump in a channel obtained using (a) first order and (b) high resolution time marching finite volume KFVS schemes

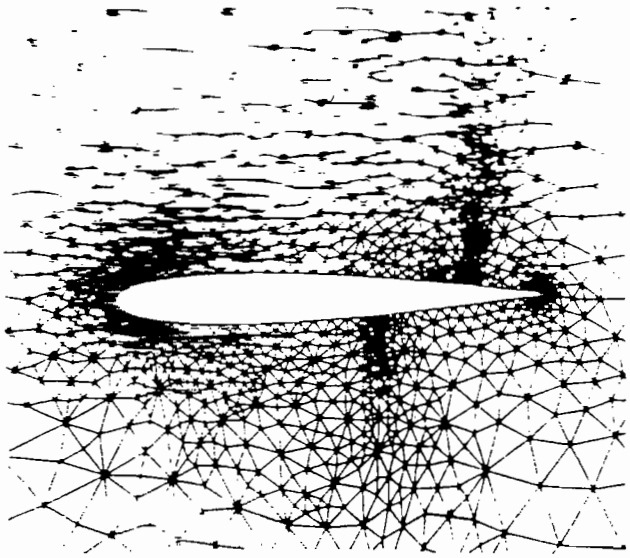

Fig 10 a Refined mesh, NACA 0012 airfoil

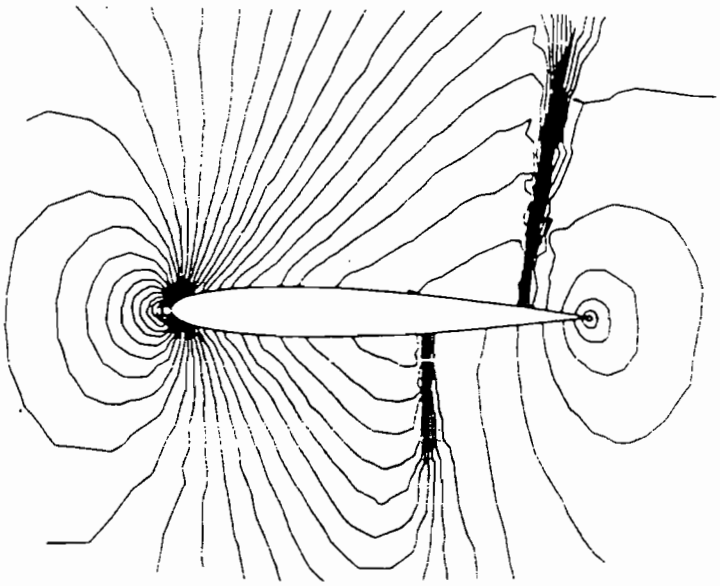

Fig 10 b Contours of pressure, refined mesh, KFVS

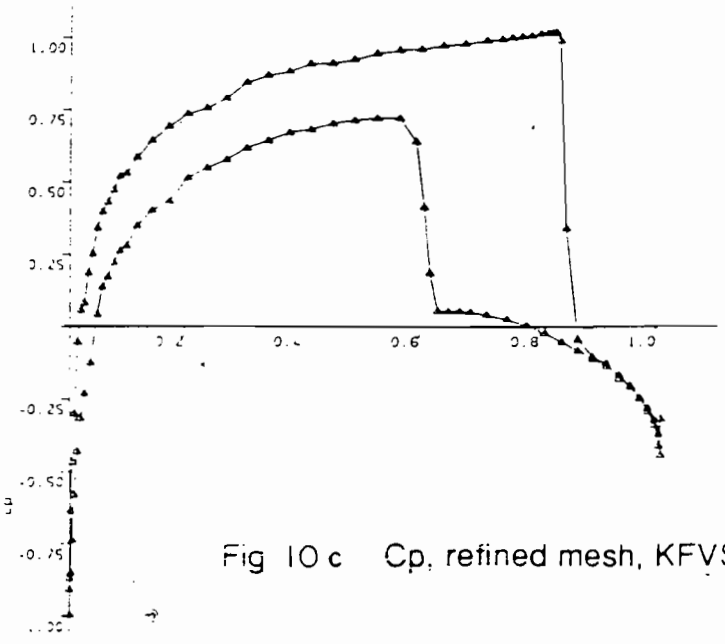

Fig 10 c Cp, refined mesh, KFVS

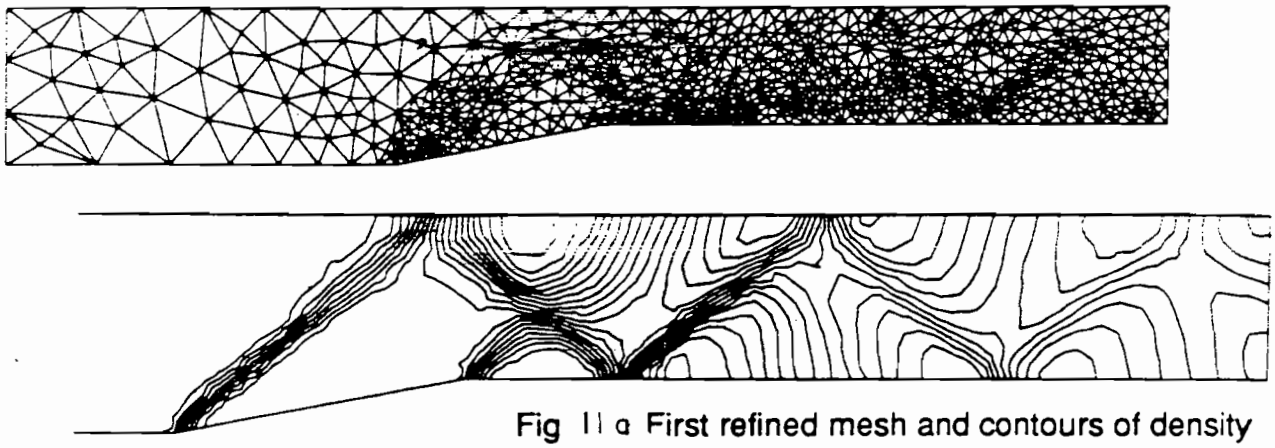

Fig 11 a First refined mesh and contours of density

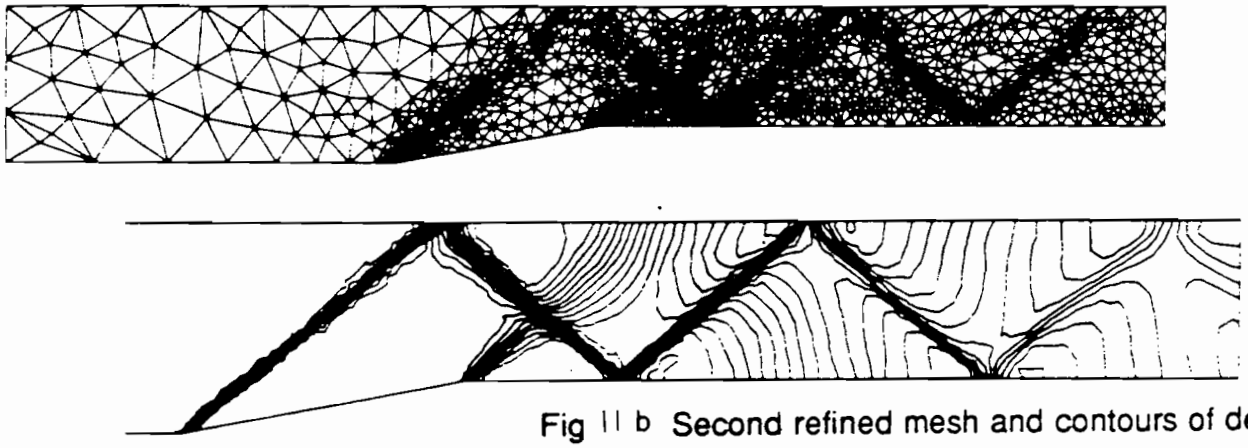

Fig 11 b Second refined mesh and contours of density

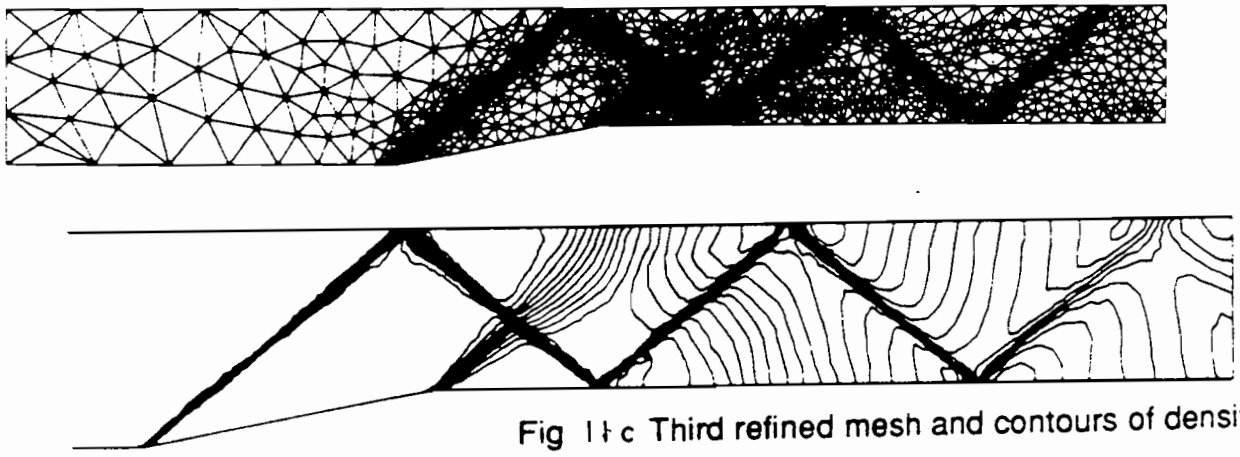

Fig 11 c Third refined mesh and contours of density

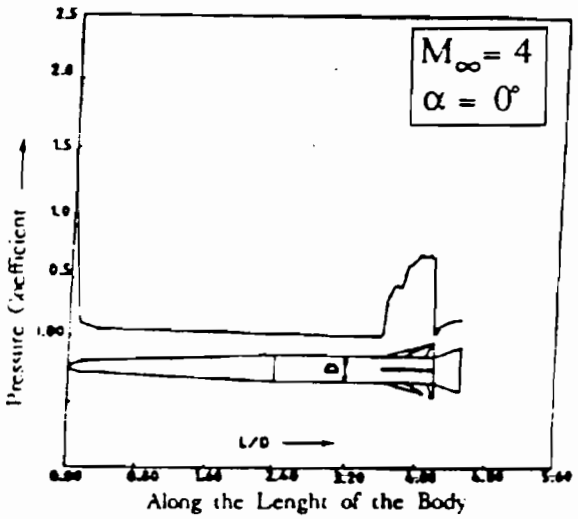

Fig. 12 Pressure distribution along blunt cone-cylinder-flare (with lifting surfaces)

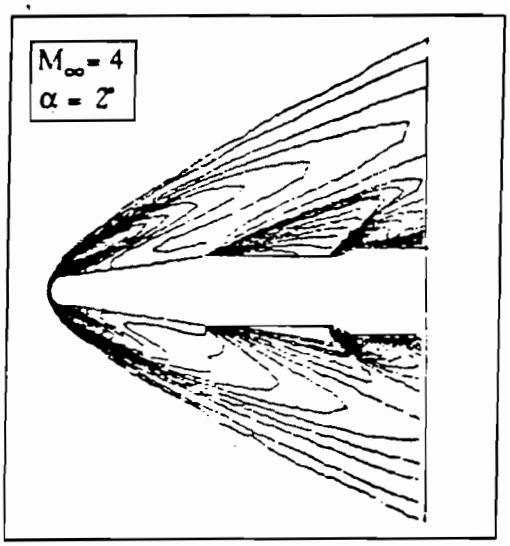

Fig. 13 Iso-pressure contours for the configuration without lifting surfaces

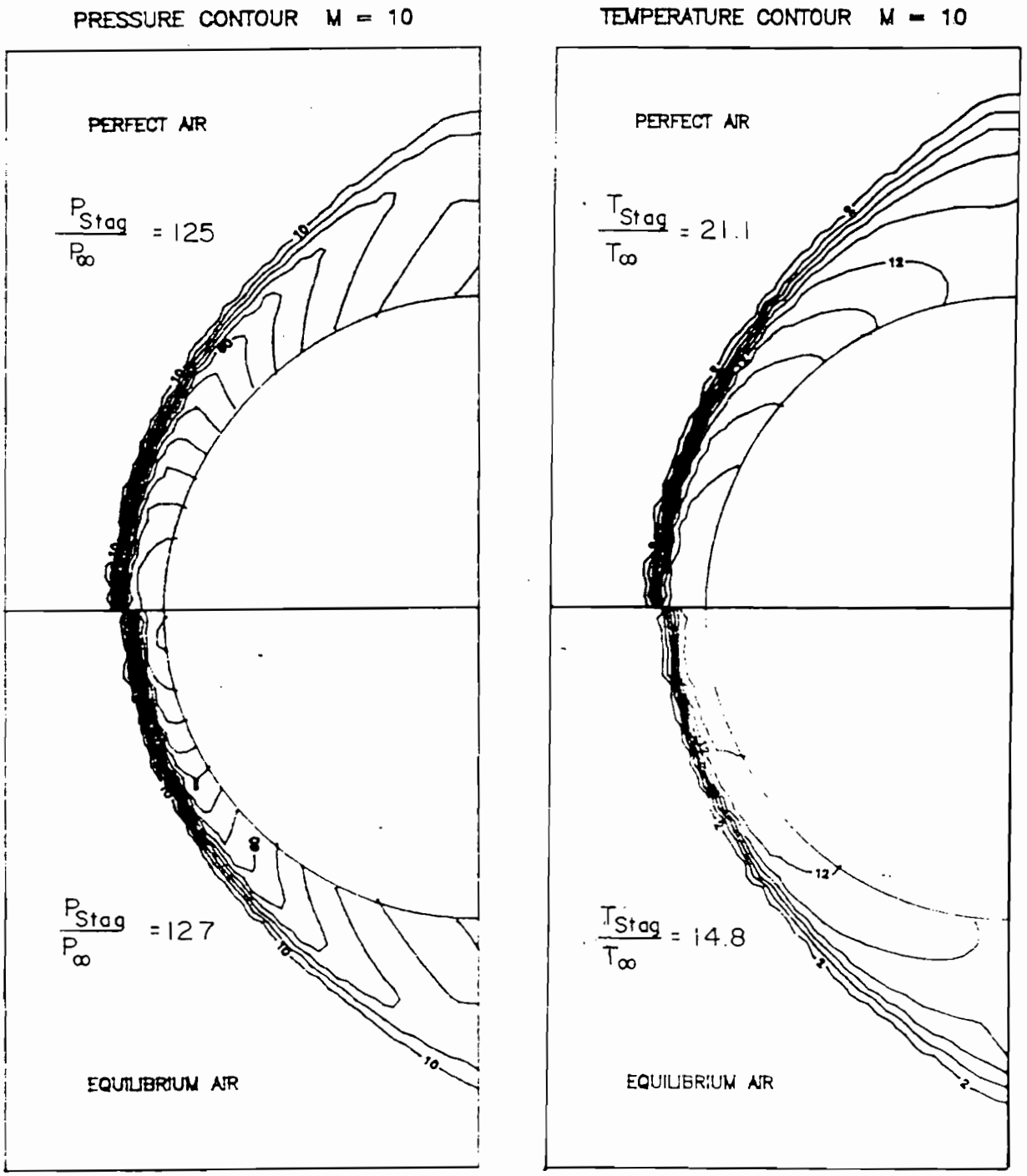

FIG.14 PRESSURE AND TEMPERATURE CONTOURS FOR REACTING FLOW PAST A SPHERE (M = 10)

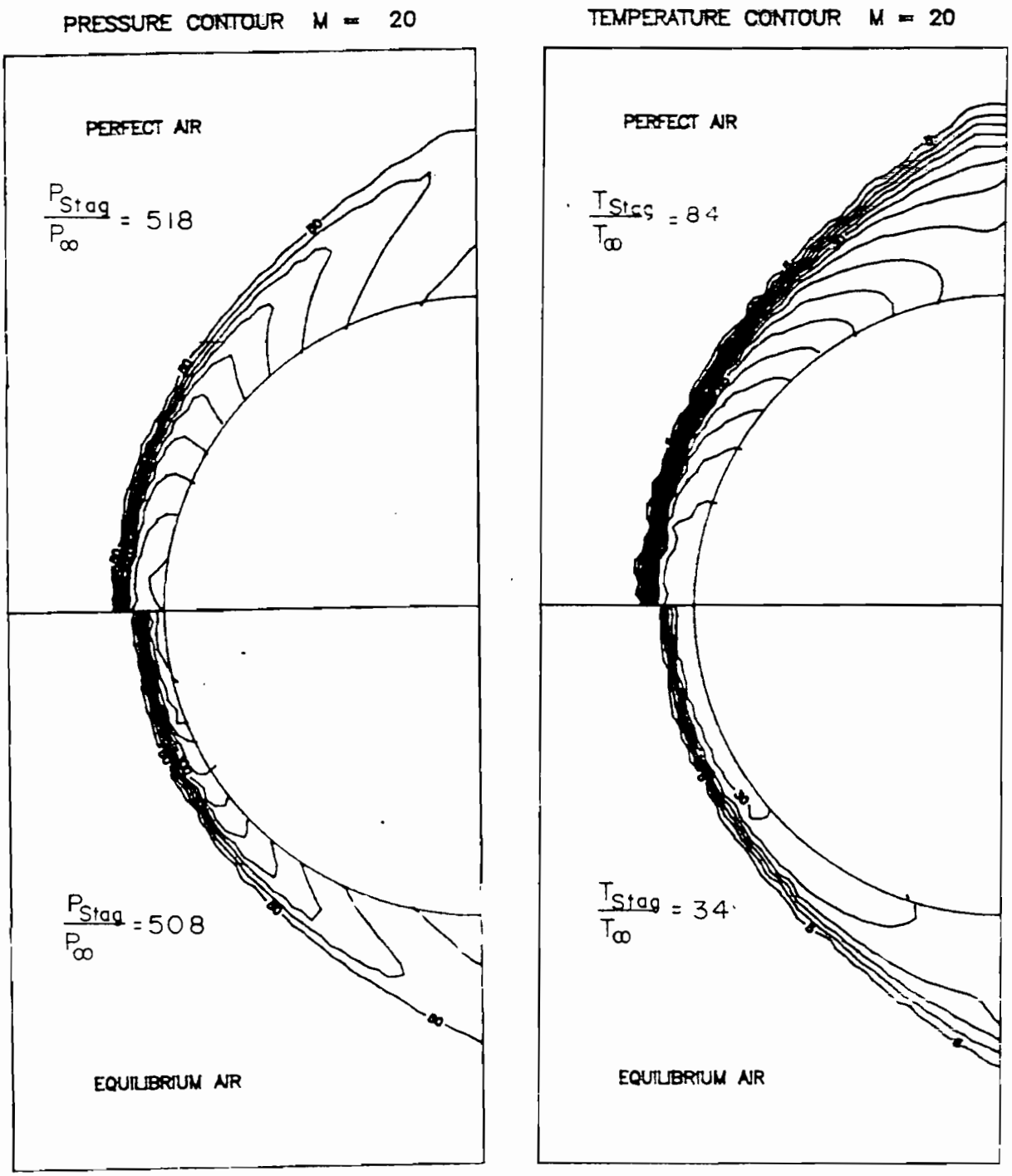

FIG.15 PRESSURE AND TEMPERATURE CONTOURS FOR REACTING FLOW PAST A SPHERE (M=20)

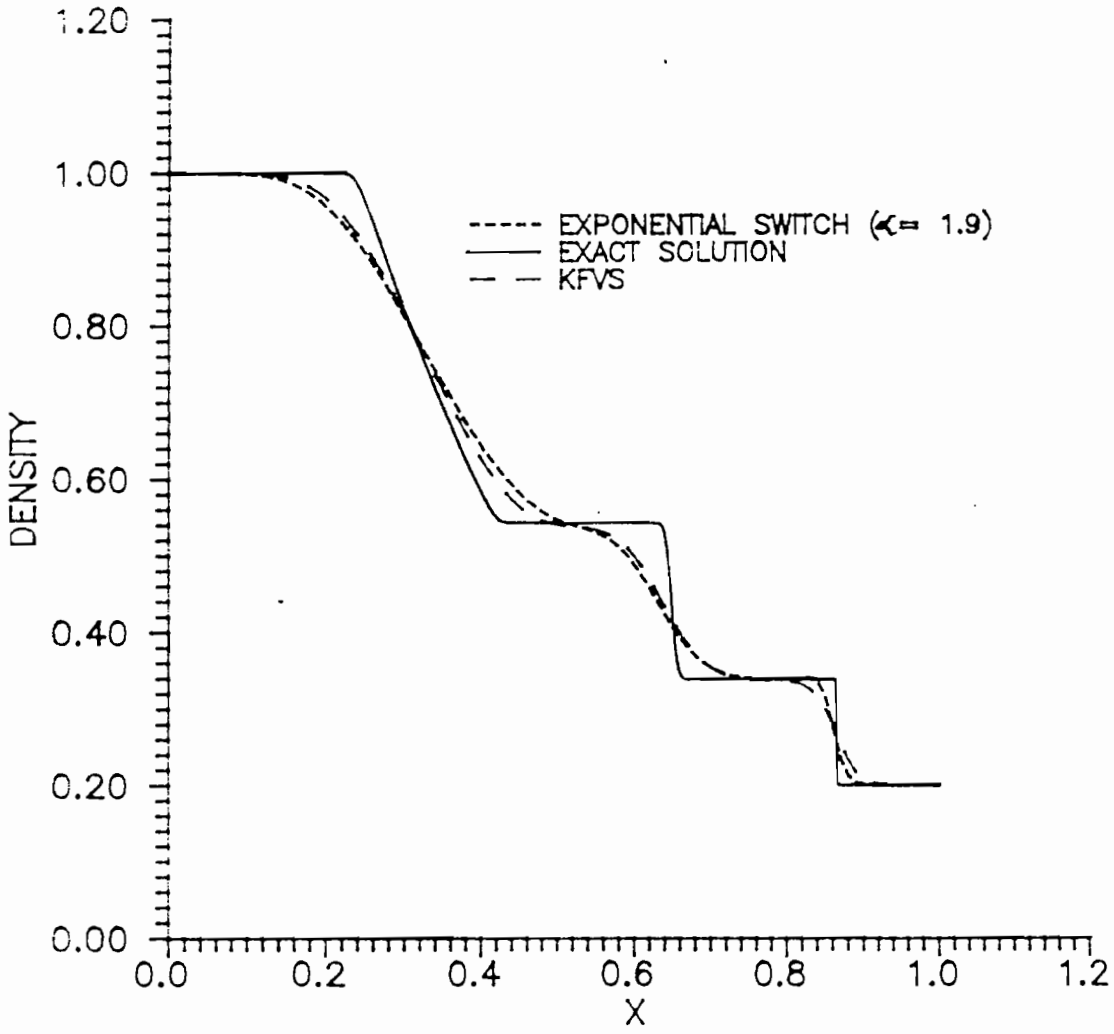

FIG.16 RESULTS FOR 1-D SHOCK TUBE PROBLEM

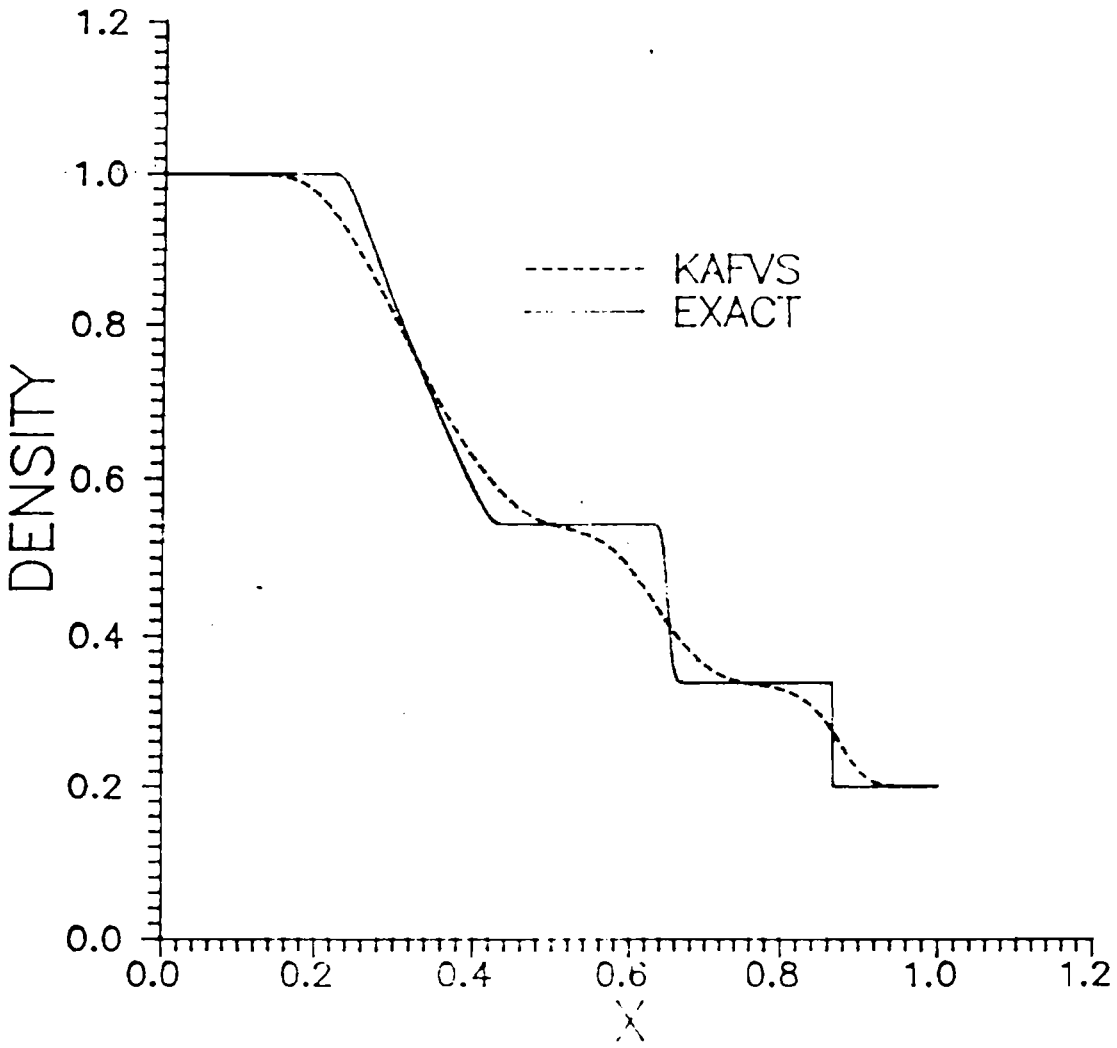

FIG. 17 RESULTS FOR 1-D SHOCK TUBE PROBLEM

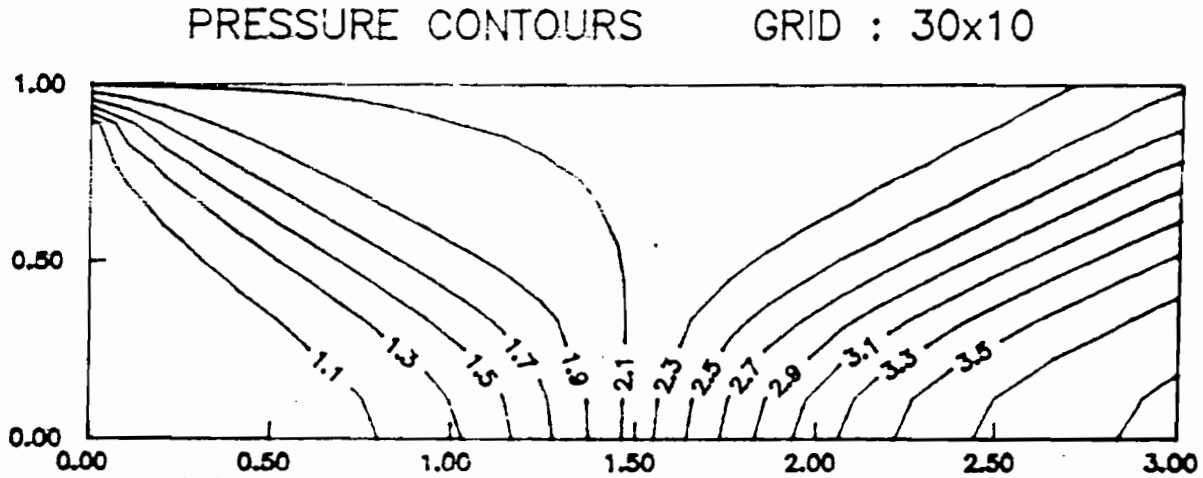

FIG. 18 (a) SHOCK REFLECTION WITH KFVS SCHEME

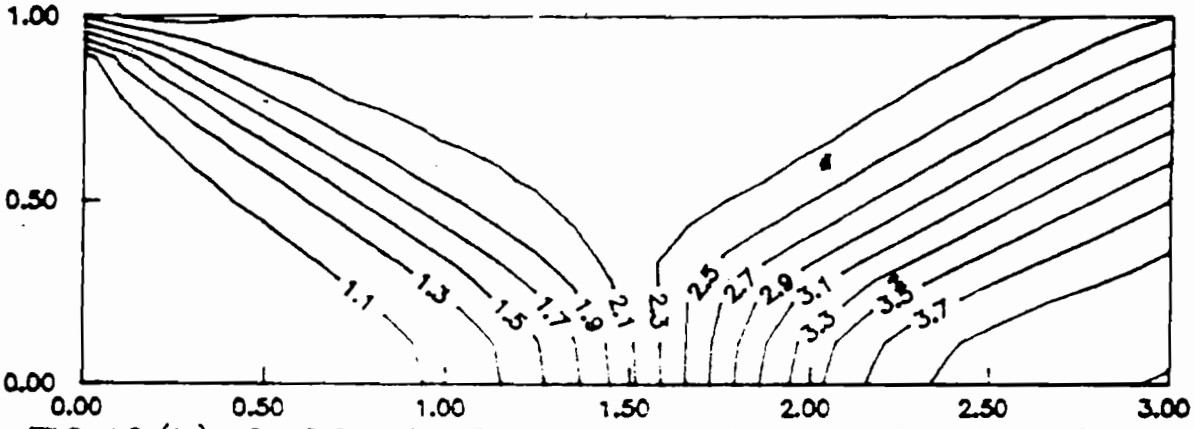

FIG. 18 (b) SHOCK REFLECTION WITH KAFVS SCHEME

OBLIQUE SHOCK REFLECTION WITH KFVS SCHEME

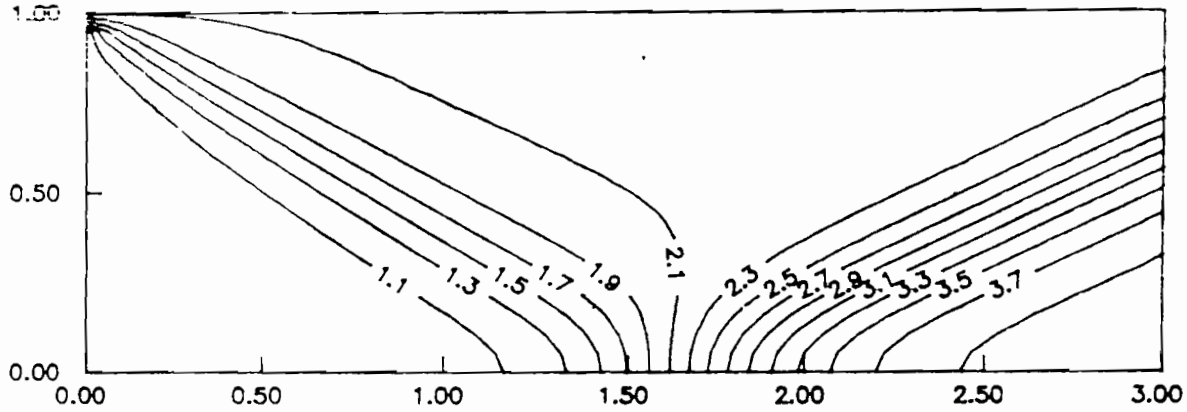

PRESSURE CONTOURS GRID : 60x20

OBLIQUE SHOCK REFLECTION WITH GMUB SCHEME

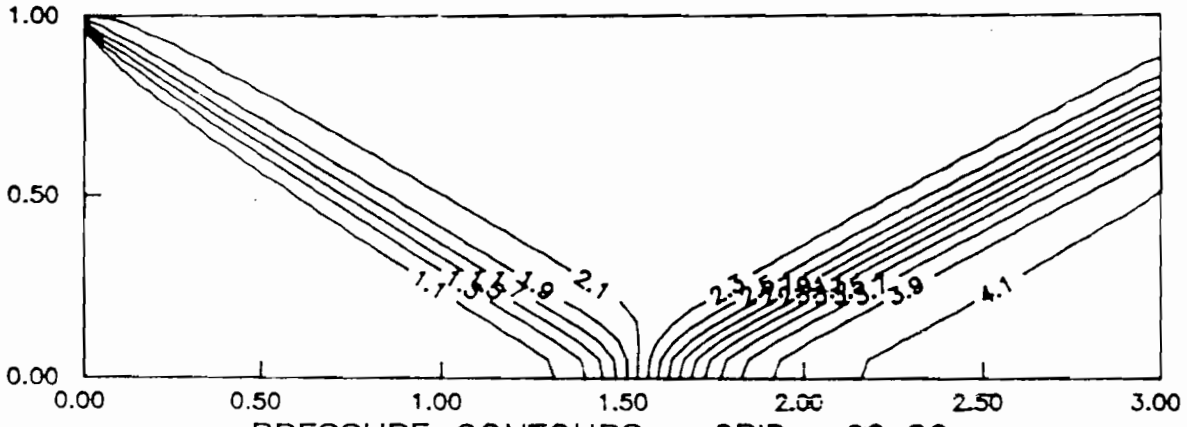

PRESSURE CONTOURS GRID : 60x20

FIG. 19

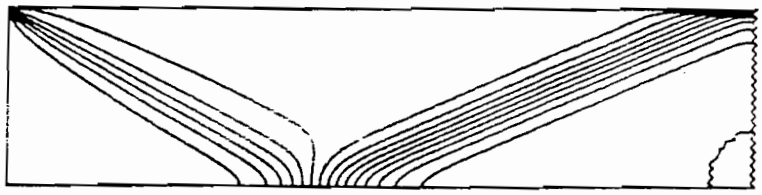

a) First order without rotation

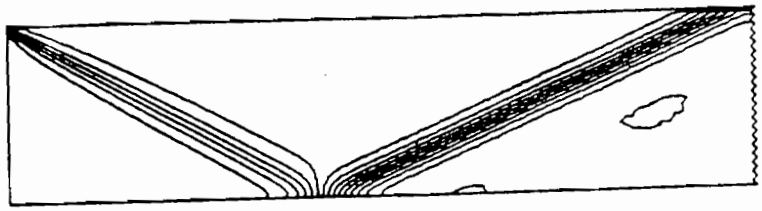

b) First order with rotation

c) Second order with rotation

Fig 20 Pressure contours for shock reflection problem using Least Squares Upwind Method.
(contour level 0.9 to 4.1 with interval 0.2)